


Cite this: *RSC Adv.*, 2021, 11, 12500

Are bacteria claustrophobic? The problem of micrometric spatial confinement for the culturing of micro-organisms†

Céline Molinaro,^{*a} Violette Da Cunha,^b Aurore Gorlas,^b François Iv,^a Laurent Gallais,^a Ryan Catchpole,^b Patrick Forterre^b and Guillaume Baffou^{*,a}

Culturing cells confined in microscale geometries has been reported in many studies this last decade, in particular following the development of microfluidic-based applications and lab-on-a-chip devices. Such studies usually examine growth of *Escherichia coli*. In this article, we show that *E. coli* may be a poor model and that spatial confinement can severely prevent the growth of many micro-organisms. By studying different bacteria and confinement geometries, we determine that the growth inhibition observed for some bacteria results from fast dioxygen depletion, inherent to spatial confinement, and not to any depletion of nutriment. This article unravels the physical origin of confinement problems in cell culture, highlighting the importance of oxygen depletion, and paves the way for the effective culturing of bacteria in confined geometries by demonstrating enhanced cell growth in confined geometries in the proximity of air bubbles.

Received 9th January 2021

Accepted 19th March 2021

DOI: 10.1039/d1ra00184a

rsc.li/rsc-advances

Introduction

The efficiency of cell culturing *in vitro* not only depends on the selection of a proper culture medium and its chemical properties, but also depends upon *physical* parameters, such as temperature, surface composition (coating, electrical charge, ...), and pressure. All these parameters have been widely investigated, well understood and generally well controlled experimentally. However, a physical parameter that has been less well-considered is spatial confinement. For some experimental methodologies, living cells need to be spatially confined over micrometre scales, such as sandwiched between two coverslips, passing through constrictions, or incorporated within a microfluidic channel.^{1,2} Microfluidic devices in particular have been increasingly used this past decade to study micro-organisms and address several biological questions, from the growth and motility of bacteria, to chemotaxis, and cellular interactions.^{3,4} Additionally, microfluidics have enabled the observation of biofilm formation,⁵ conjugation between strains,⁶ and new insights into bacteria-mediated cancer therapies.⁷ A valuable feature of microfluidic devices is the possibility to create local chemical gradients, facilitating studies of bacterial chemotaxis.⁸ Furthermore, spatial constrictions like

micropores can enable the selective passage of bacteria, or the observation of their behaviour within a maze.^{9,10} Very thin, elongated constrictions can also be used to spatially organize bacteria over the field of view of a microscope and achieve easy statistical characterization of a large number of cells.¹¹

It is notable that most of these studies utilizing spatial confinements were carried out with *Escherichia coli* bacteria as a model species, which is indeed recognized as suited for culture in confined geometries. For instance, the growth rate of *E. coli* was shown to be equivalent in micron-sized channels and in suspension,¹² with a no-growth threshold around 0.5 μm .¹³ Männik *et al.*¹⁴ compared the growth and motility of *E. coli* (Gram-negative) and *Bacillus subtilis* (Gram-positive) in micro-fabricated channels, showing that *E. coli* can grow in narrower channels than *B. subtilis* thanks to its thin Gram-negative cell wall. Only a handful of other prokaryotic species have been investigated in similar confinements. For instance, *Halobacterium salinarum*, an archaeon, can grow in 1.3 μm high and 10 μm long cavities, albeit with a generation time three times longer than in suspension.¹⁵ We speculate that the predominance of *E. coli*-based literature involving microfluidic channels may come from the inability of many micro-organisms to grow in reduced spaces, though this is not stated in the literature.

In this article, we evidence the inability of different bacteria to grow in confined geometries and unravel the origin of this growth inhibition. We show that *Escherichia coli* and *Lactobacillus reuteri* can easily divide in confined geometries (<20 μm), while *Thermus thermophilus* and *Geobacillus stearothermophilus* are unable to grow below a spatial confinement of around 300 μm . The results indicate that this claustrophobic behaviour

^aInstitut Fresnel, CNRS, Aix Marseille University, Centrale Marseille, Marseille, France. E-mail: celine.molinaro@fresnel.fr; guillaume.baffou@fresnel.fr

^bUniversité Paris-Saclay, CEA, CNRS, Institute for Integrative Biology of the Cell (I2BC), 91198, Gif-sur-Yvette, France

† Electronic supplementary information (ESI) available. See DOI: 10.1039/d1ra00184a



results from depletion of dioxygen in small volumes, not from nutrient deficiencies, as confinement only affected the growth of aerobic bacteria. This hypothesis is further supported by the ability of the aerobic bacteria to grow in confined geometries, provided an air bubble is present nearby. A last section provides numerical simulations confirming the strong reduction of bacterial growth and oxygen depletion with the geometry used in this study.

Results and discussion

During microscopic culturing experiments, we noted a striking inhibition of growth of several bacterial species when deposited between glass coverslips, typically separated by $<100\ \mu\text{m}$. To demonstrate the issue and uncover its causal origin, we conducted experiments on 4 species of bacteria (listed in Table 1) in 3 geometries. These bacteria were selected for their short generation time ($<45\ \text{min}$) and for their oxygen requirement. The 3 types of geometries correspond to the three following sections.

Growing bacteria in $<20\ \mu\text{m}$ thin layer

We first demonstrate the ability/inability of bacteria to grow in confined geometries. Bacterial species depicted in Table 1 were cultured separately, sandwiched between two coverslips, in a $20\ \mu\text{m}$ thick liquid medium. The top coverslip was cut to be smaller than the bottom one, so that only part of each culture was covered. As such, some bacteria of a given culture were spatially confined, while others were not. Videos were acquired over several hours at the edge of the coverslip, to capture both confined and unconfined bacteria within a single field of view of the microscope (Fig. 1).

Under these conditions, *E. coli* grew normally both under the coverslip and in open space with a similar generation time (see Movie Ecoli.mov in ESI† from which images in Fig. 1a–c have been extracted). This result is consistent with the many effective studies reported on *E. coli* bacteria in confined geometries^{11–13} (as discussed in above). We reproduced the same experiments with *L. reuteri* (Fig. 1d and f), which also displayed growth both under the coverslip or in open space with a similar generation time (see Movie LactobacillusR.mov in ESI†). In contrast, results obtained with the aerobic bacteria *G. stearothermophilus* (Fig. 1g and i) revealed a completely different behaviour (see Movie GeobacillusS.mov in ESI†). Substantial growth was observed on the open side, with complete growth inhibition in the $20\ \mu\text{m}$

thick medium layer. Furthermore, spatially confined *G. stearothermophilus* adopt a spherical geometry reminiscent of sporulation. *T. thermophilus*, another strictly aerobe, exhibited the same behaviour: the total inability to grow in confined geometry (Fig. 1j and l). *T. thermophilus* grows as long filaments observable in the uncovered portion of the cultured slides (Fig. 1k and l). In contrast, similar filamentous cells do not develop when covered (see the associated Movie Thermus-T.mov in ESI†).

Claustrophobic behaviour as a function of the media layer thickness

The previous section demonstrates the inability of some bacteria species, *G. stearothermophilus* and *T. thermophilus*, to grow in a $20\ \mu\text{m}$ thick medium, while they can grow in open medium. The natural question is to determine the maximum degree of spatial confinement to which this problem persists. For the two species of bacteria that suffer when confined, *G. stearothermophilus* and *T. thermophilus*, samples were prepared with liquid thicknesses of $120\ \mu\text{m}$, $360\ \mu\text{m}$, $600\ \mu\text{m}$, $840\ \mu\text{m}$ and $1\ \text{mm}$ (by stacking $120\ \mu\text{m}$ spacers, see Methods section). Each sample contained the initial same amount of bacteria (equal optical density (OD) and solution volume).

The results obtained with *G. stearothermophilus* are displayed in Fig. 2. Similar to that observed above (Fig. 1h and i), a sporulation-like phenotype was observed after 2 h of incubation at $120\ \mu\text{m}$ and $360\ \mu\text{m}$ liquid thickness. Sporulation typically indicates unfavourable growth conditions, suggesting spatial confinement is poorly tolerated by this species. In contrast, above $360\ \mu\text{m}$ effective growth was observed at both 2 h and 3 h. A similar behaviour was observed for *T. thermophilus*, that is no growth below $360\ \mu\text{m}$ of medium thickness, and effective growth at $360\ \mu\text{m}$ and above (Fig. 3). *T. thermophilus* bacteria required more time to demonstrate effective growth, around 4 h of incubation. In both cases, thicker liquid medium facilitated faster growth of bacterial cells.

Growth close to air bubbles despite of confinement

We demonstrated above that only the two facultative anaerobes we studied could blossom in confined environments. These results suggest growth inhibition may be caused by a lack of dioxygen in confined environments. Beyond oxygen depletion, other explanations of the growth inhibition in confined geometries could have been a rapid depletion of a nutrient present in the medium due to consumption by the cells, an accumulation of inhibitory waste compounds, or a depletion of

Table 1 Bacterial species used in this work, along with their aero/anaerobic property and generation time

Bacterial species	Metabolic description	Generation time	Gram stain
<i>Escherichia coli</i>	Facultative anaerobe	15–20 min	Gram-negative
<i>Lactobacillus reuteri</i>	Facultative anaerobe	~45 min	Gram-positive
<i>Thermus thermophilus</i>	Strictly aerobe	20 min	Gram-negative
<i>Geobacillus stearothermophilus</i>	Strictly aerobe	25 min	Gram-positive



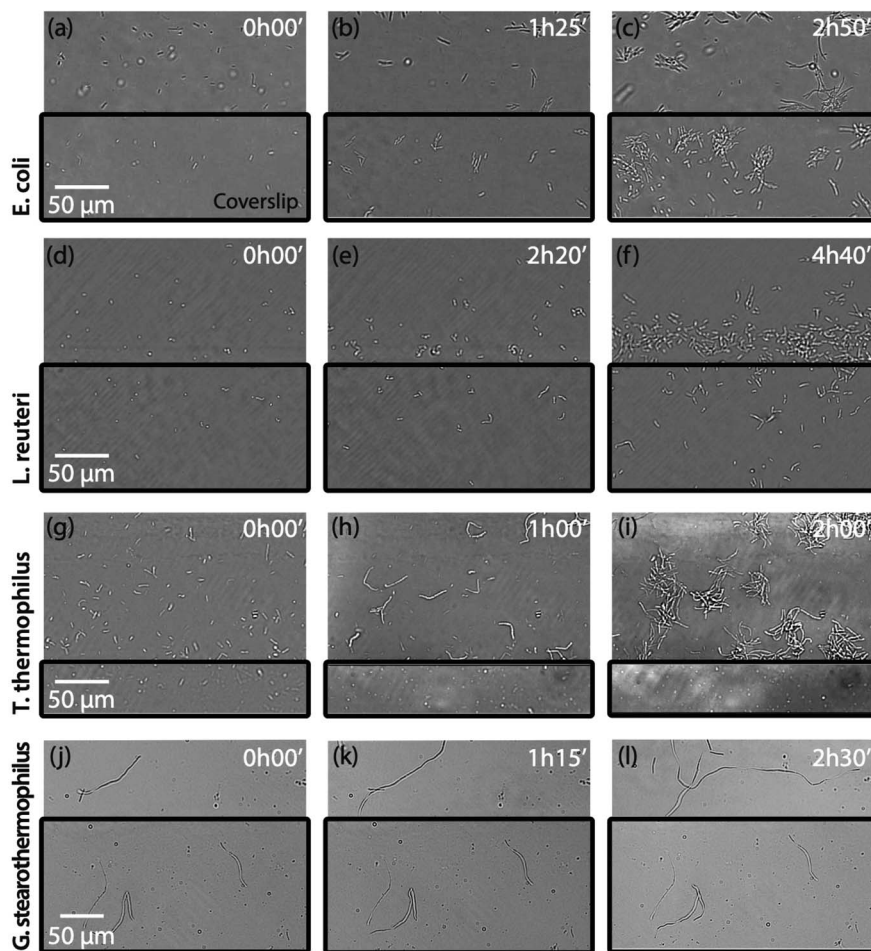


Fig. 1 (a–c) Images of the growth of *E. coli* at 37 °C, at 0 h, 1 h 25 min and 2 h 50 min. (d–f) Images of the growth of *Lactobacillus reuteri* at 35 °C, at 0 h, 2 h 20 min and 4 h 40 min. (g–i) Images of the growth of *Geobacillus stearothermophilus* at 60 °C, at 0 h, 1 h and 2 h. (j–l) Images of the growth of *Thermus thermophilus* at 70 °C, at 0 h, 1 h 15 min and 2 h 30 min. In all the images, the top coverslip lies on the bottom part, represented as a thick, black solid line.

nutriments due to electrostatic affinity with the naturally negatively charged glass surface. However, none of these mechanisms would be consistent with an active growth close to air bubbles. Gas bubbles can only affect the nearby gas content of the liquid. The hypothesis of oxygen depletion was confirmed here by the observation that effective growth of *G. stearothermophilus* and *T. thermophilus* was possible in the presence of nearby trapped air bubbles, despite confinement in 120 μm thick culture medium (Fig. 4a and f). By underfilling the sample well, an air/medium interface can be trapped within the coverslip-confined region and observed within the microscope field. The presence of this interface allowed growth of *G. stearothermophilus* in the vicinity, and even several 100 μm away. Despite the 120 μm thick culture medium, this growth was even faster than the growth observed in the 1 mm confinement tests (Fig. 4a and c vs. Fig. 2m and 2o). Additionally, the sporulation-like phenotype was absent close to the air layer (Fig. 4b vs. Fig. 1i).

Similar behaviour was observed with *T. thermophilus* in a 120 μm thick culture medium, this time illustrated with a trapped

air bubble (Fig. 4d–f). Here again, effective bacterial growth is observed in the proximity of the air bubble. Additionally, over the course of 4 h, the bubble reduced in size, consistent with oxygen consumption by the bacteria. For both experiments, images were recorded from the same sample but away from the air layer or bubble. No growth was observed for both types of bacteria anywhere else in the sample (Fig. S2 and S3†).

Air layers or bubbles behave as constant, long sources of dioxygen, allowing continued diffusion from the gas to the liquid. Gas content is the only medium property expected to vary at the vicinity of an air interface, which confirms the hypothesis of dioxygen depletion, and/or carbon dioxide increase, as the origin of the deleterious effect and apparent claustrophobic behaviour of aerobic bacteria: bacteria are actually suffocating in confined geometries.

Estimation of oxygen consumption in confined geometries

As a further support of the suffocation mechanism, we determine here the time needed for the bacteria to consume the



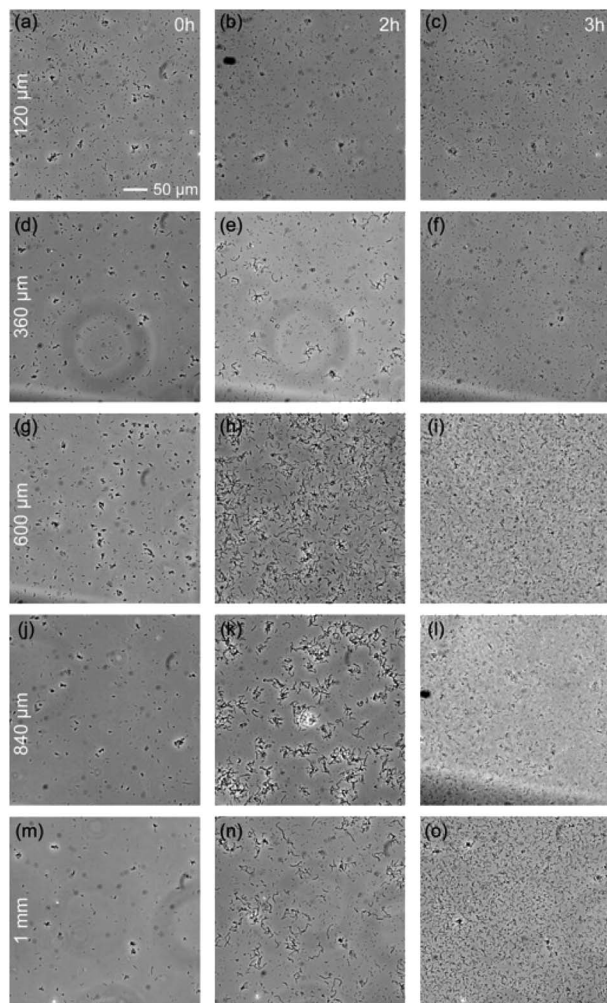


Fig. 2 Phase-contrast images of *Geobacillus stearothermophilus* for various liquid thickness, from 120 μm to 1 mm (a, b, and c) to (m, n, and o), after 0 h, 2 h and 3 h (columns) of incubation at 60 $^{\circ}\text{C}$, over the same area.

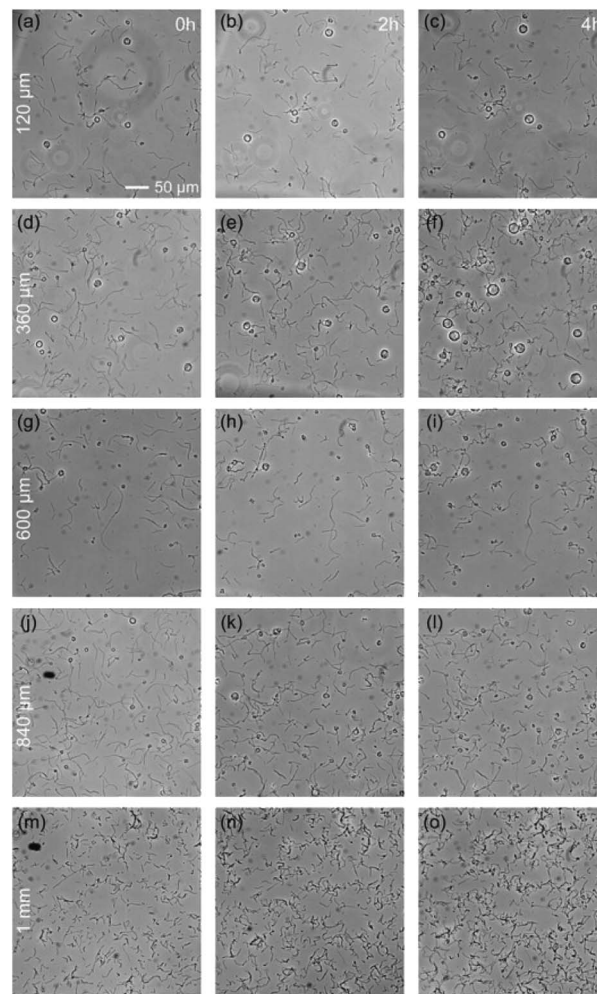


Fig. 3 Phase-contrast images of *Thermus thermophilus* for various liquid thickness, from 120 μm to 1 mm (a, b, and c) to (m, n, and o), after 0 h, 2 h and 4 h (columns) of incubation at 70 $^{\circ}\text{C}$, over the same area.

dioxygen contained in the confined volume in which they are living.

We first consider the case of a spatial confinement in a SecureSeal spacer ($h = 120\ \mu\text{m}$ in thickness, and $S = \pi 4.5^2\ \text{mm}^2$ in area), for which the oxygen consumption can be simply estimated without numerical simulations. To the best of our knowledge, no measurement of dioxygen consumption of *G. stearothermophilus* or *T. thermophilus* have been reported in the literature. Typical values of dioxygen molecule consumption rate per bacteria Q_0 found in the literature for other bacteria,^{16,17} including *E. coli*, lie in the range of $Q_0 = 3 \times 10^{-19}$ to 3×10^{-18} mol per second per cell, representing a consumption of 2×10^5 to 2×10^6 molecules per second per cell. In the experiment reported above, for the case of a 120 μm spacer, we used $V = 7\ \mu\text{L}$ of bacterial suspension, with an OD of 0.08 corresponding to $n_b = 2 \times 10^8$ cell per mL, leading to a cell areal density of $\sigma_b = n_b h = 2.4 \times 10^{10}$ cell per m^2 on the bottom coverslip. In 7 μL of water at 25 $^{\circ}\text{C}$, with $\rho_{\text{O}_2} = 8.28\ \text{mg L}^{-1}$ of

dissolved dioxygen, there is $n_0 = 1.8 \times 10^{-9}$ moles of O_2 . All the dissolved dioxygen is to be consumed over a time scale $\tau = \rho_{\text{O}_2} h / Q_0 M_{\text{O}_2} \sigma_b$, where M_{O_2} is the molar mass of O_2 . Giving the typical range of O_2 consumption rate Q_0 given above, it yields a time scale τ ranging from 6 minutes to 1 hour. This range means that after a few minutes or tens of minutes, the oxygen content of the sample should be significantly reduced, hampering the proper development of strictly aerobic bacteria. This estimation is consistent with the experiments we conducted.

Then, we address the more complex case of a bacteria culture partly covered by a coverslip (Fig. 1). We conducted numerical simulations using Comsol Multiphysics to model the whole 3-dimensional (3D) problem (the Comsol file is provided in ESI†). Fig. 5 provides an overview of the results. The system is composed of a coverslip creating a 15 μm thick medium layer on half of a 2-dimensional culture of bacteria (Fig. 5a). A 1 mm thick liquid medium is covering the whole system. The simulations involve variations of the O_2 concentration in 3D, and variations of the bacteria population as a function of their



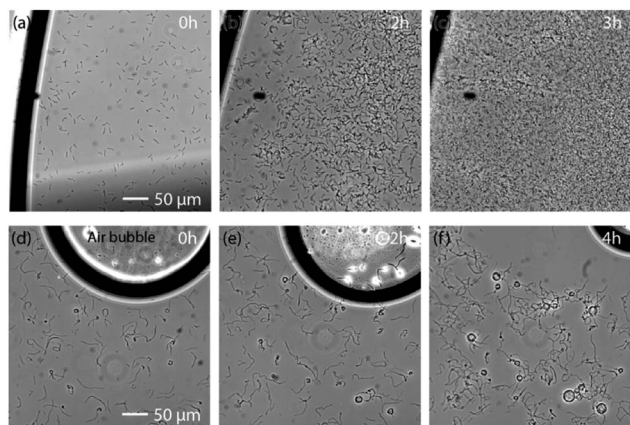


Fig. 4 Phase-contrast images of *G. stearotherophilus* after (a) 0 h, (b) 2 h and (c) 3 h of incubation at 60 °C. All the images correspond to the same location within the sample. The air layer is on the left side of each image demarcated by the thick black line. Phase-contrast images of *T. thermophilus* after (d) 0 h, (e) 2 h and (f) 4 h of incubation at 70 °C. Images display the same location within the sample. An air bubble, located at the top-right corner of each image, was trapped in the suspension, shrinking over time.

dioxygen consumption over time (the list of the different parameters and details on the theory can be found in the Methods and Materials section). The Comsol program provided in ESI† can be used to further vary all the parameters.

Fig. 5b gives an overview of the 3D distribution of O_2 concentration in the system after 1 h 30 min of incubation. A substantial dioxygen depletion is observed below the coverslip.

Note that the system is invariant along the x axis. The linear spatial profile of O_2 concentration on the bottom of the chamber is plotted in Fig. 5d, at different times. After only 20 min a substantial depletion of oxygen is observed below the coverslip (blue curve in Fig. 5d). Fig. 5c represents the bacterial density on the bottom of the chamber after 1 h 30 min of incubation. While bacteria have been actively growing in the open medium, their development is seriously hampered under the coverslip. The linear profile of the normalized bacterial density σ_b/σ_0 in Fig. 5e plots the evolution of the linear profile over time, and evidences almost no bacterial growth after a few 100 s of μm from the border of the coverslip, under the coverslip. The evolution over time of O_2 concentration and bacterial density are represented in Fig. 5f and g, at different positions along the y axis. A substantial decay of oxygen concentration is rapidly observed below the coverslip. All these results are consistent with our experimental observations, although what we actually measured is a bit worth in term of bacterial growth below the coverslip. This may be due to the fact that the bacteria exhibit a latency phase, where they consume oxygen without growing. Also, we hypothesize in our model (see theory in Methods and Materials section) that the bacterial growth is proportional to the oxygen concentration. A more reasonable assumption would be that below a certain oxygen concentration, growth is inhibited. This would yield a further reduction of the bacterial growth.

Water in equilibrium with the atmosphere contains around 10^5 dioxygen molecules per μm^3 (c_0). This number seems unrealistically large, but an aerobic bacterium is consuming around 1 million dioxygen molecules per second (Q_0). Bacteria are thus very effective oxygen consumers, despite their small

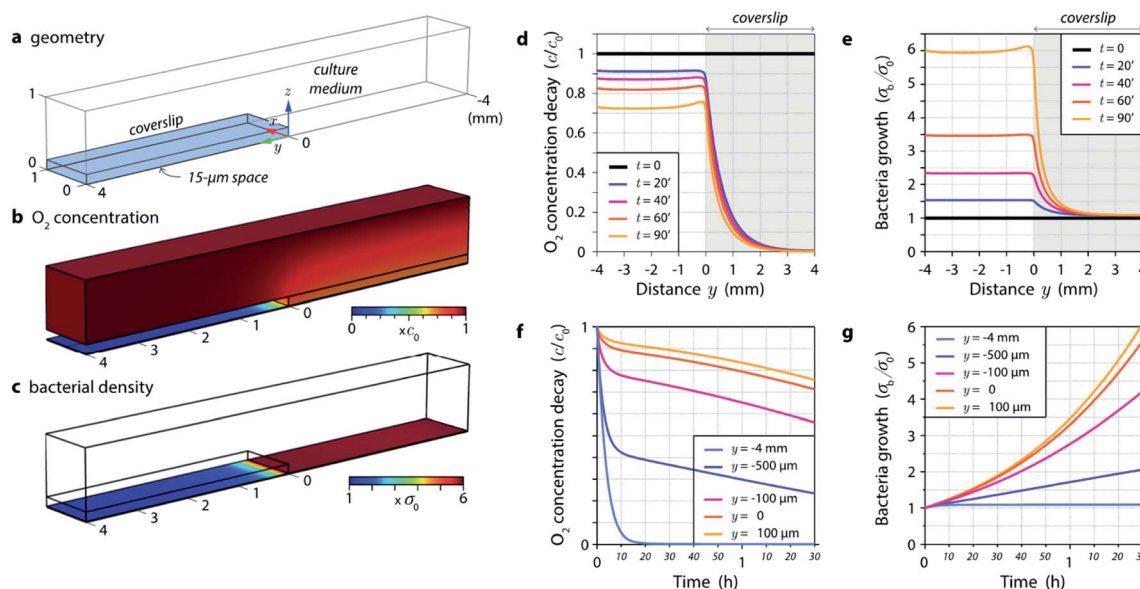


Fig. 5 (a) Geometry of the system investigated numerically, consisting of a glass coverslip partly covering a bacterial culture. (b) Dioxygen concentration plotted in 3 dimensions at $t = 1$ h 30 min. (c) Bacteria areal density at $t = 1$ h 30 min. (d) Linear profile of the bacterial density along the y axis at different times (from 0 to 1 h 30 min). (e) Linear profile of the O_2 concentration along the y axis at $z = h/2$, at different times. (f) Evolution of the bacterial density at different positions along the y axis. (g) Evolution of the O_2 concentration at different positions along the y axis, at $z = h/2$.



size. In the meantime, oxygen diffuses extremely slowly in water (D_{O_2} around $0.001 \text{ mm}^2 \text{ s}^{-1}$), which explains why spatial restriction hampering efficient oxygen diffusion could seriously affect this extreme need of oxygen consumption.

Conclusions

We demonstrate that spatial confinement below a few hundred micrometres prevents the growth of aerobic bacteria. By measuring the growth of 4 bacterial species (two facultative anaerobes and two strictly aerobes) under such conditions, we demonstrate that this phenomenon is unique to the strictly aerobic species. We hypothesized that this growth inhibition was due to fast oxygen consumption and depletion. In support of this hypothesis, we show that growth of aerobic cells can be restored in the vicinity of trapped air bubbles, even under confinement conditions. Not only do these results provide evidence toward the origin of the problematic growth we observed (oxygen depletion), it also provides a convenient approach to enable aerobic bacteria culture under confined geometries, such as microfluidic devices. We recognize that the origin of the claustrophobic behaviour may not be evident. In particular, a possible explanation could have been rapid depletion of a nutriment present in the medium due to consumption by the cells, or accumulation of inhibitory waste compounds. Additionally, this effect could be synergistic with rapid hypoxia resulting in accumulation of by-products from anaerobic metabolism, or depletion of nutriments preferred in hypoxic conditions. Also, if some nutriments had electrostatic affinity with the naturally negatively charged glass surface, it could lead to an effective removal of these compounds from the culture medium bulk, or even pH modification. This mechanism would be favoured by the presence of the two glass coverslips and the sandwich geometry, characterized by a very high glass-surface/medium-volume ratio, which does not occur with a single coverslip. The results presented in this study challenge any such variations of the chemical nature of the culture medium as a possible explanation of the problem. A lack of dioxygen was evidenced as the sole origin of the problem. Bacteria are actually suffocating in confined geometries.

Methods and materials

Bacteria growth conditions

Escherichia coli (HST08 – Stellar) were grown at 37°C , 200 rpm in LB media (LB broth 1231 – Conda). *Lactobacillus reuteri* (DSM 20016) were grown at 35° , 200 rpm in MRS culture media (MMRS broth 69966 Sigma-Aldrich and tween 80 P8074 Sigma-Aldrich). *Thermus thermophilus* (CIP 110185T, type strain HB8) were grown at 70°C , 200 rpm in LB media. *Geobacillus stearothermophilus* were grown at 60°C , 200 rpm in LB media. For each experiment, cultures were grown overnight. The optical density (OD) was then measured with a spectrophotometer (Ultrospec 10 – Biochrom) and adjusted to the required OD (600 nm).

20 μm confinement experiments

A VAHEAT heating stage (Interference) with their PDMS (polydimethylsiloxane) reservoirs was used to set the temperature of the culture (Fig S1†). Observations were performed with a $40\times$ air-objective (Olympus). To avoid excess convection and heat shock, heating was performed gradually ($\sim 0.05^\circ\text{C s}^{-1}$). Experiments were conducted at least in triplicate for each bacterial strain. In each experiment, $0.2 \mu\text{L}$ of bacterial suspension (OD 0.3) was dropped in the VAHeat reservoir and immediately covered by a small $150 \mu\text{m}$ thick coverslip with a triangular shape. This top coverslip was fabricated by a glass laser cutting technique. The laser processing system is based on a commercial femtosecond-diode-pumped ytterbium amplified laser source (S-Pulse HP, Amplitude Systemes) operating at 1030 nm (FWHM 5 nm) with a spatially Gaussian beam profile. The source is coupled in a dual-axis scanning galvanometric system (GVS012/M, Thorlabs) with metallic mirrors and a 100 mm focal length f-theta lens (FTH100-1064, Thorlabs). The $150 \mu\text{m}$ thickness coverslips were processed with the following parameters: beam diameter $60 \mu\text{m}$, repetition rate 1 kHz, 0.5 mJ energy per pulse, $10 \mu\text{m}$ steps.

Varying thicknesses experiments

To create cavities of various thicknesses, we used spacers, 1 mm thick (Press-to-seal Silicone Isolator, P24744, Invitrogen) and $120 \mu\text{m}$ thick (SecureSeal Imaging spacer, GBL654008, Sigma-Aldrich). The $120 \mu\text{m}$ spacers have been stacked to gradually vary the thickness from $120 \mu\text{m}$ to $840 \mu\text{m}$. The same volume ($7 \mu\text{L}$ – OD 0.08) of bacterial suspension was deposited in each seal. Each well was then completely filled with the appropriate culture media, and hermetically sealed with a glass coverslip. After a sedimentation time (from 1 h 30 min to 20 h depending on the strain and on the well thickness), the samples were incubated at the appropriate growth temperature without shaking. Images of the sample were taken just before incubation (0 h) and then every hour with a CMOS camera (DCC1545M-GL – Thorlabs) plugged to an inverted phase-contrast microscope (Eclipse TS2 – Nikon, $10\times$ objective). A mark was placed on each sample to observe the same area throughout the experiment. Only *Geobacillus stearothermophilus* and *Thermus thermophilus* were studied this way.

Bubble experiments

The growth of bacteria was monitored in the vicinity of air in order to validate the hypothesis of claustrophobia due to weak dioxygen renewal. $120 \mu\text{m}$ thick spacer were stuck on cleaned glass cover slides. $5 \mu\text{L}$ of bacterial suspension (OD 0.08) was deposited in each seal. Then, the $120 \mu\text{m}$ thick spacer was enclosed with a glass coverslip. The seals were not complete, with a thin layer of air between the spacer and the suspension. Air bubbles trapped randomly inside the suspension droplet were observed (Fig. 4). After waiting 1 h 30 min for sedimentation, samples were incubated at 60°C for *Geobacillus stearothermophilus* and 70°C for *Thermus thermophilus*. Images of the sample were taken just before incubation (0 h) and then



every hour with a CMOS camera plugged to an inverted phase-contrast microscope. Experiments were performed at least in triplicates.

Comsol simulations

Here are the parameters used in the simulations:

Parameters	Value	Unit	Definition
H	1	mm	Height of the chamber
W	1	mm	Width of the chamber
L	4	mm	Length of the chamber
h	15	μm	Height of the confinement
e	150	μm	Thickness of the coverslip
Q_0	10^6	s^{-1}	Bacterial O_2 consumption
c_0	1.5×10^{23}	m^{-3}	Initial O_2 concentration
σ_0	10^{10}	m^{-2}	Initial bacterial density
D_{O_2}	2×10^{-9}	$\text{m}^2 \text{s}^{-1}$	Dioxygen diffusivity
τ	30	min	Bacterial generation time

The model used in the Comsol simulations involved the diffusion law in 3 dimensions for the oxygen concentration c :

$$D_{\text{O}_2} \nabla^2 c = \partial_t c.$$

A boundary condition has to be applied to this differential equation, on the bottom of the chamber, where the bacteria are deposited, as a negative source term removing oxygen from the medium:

$$J = -Q_0 \sigma_b \frac{c}{c_0}$$

The other boundary condition of the problem is the setting of $c = c_0$ on the top of the chamber.

Finally, the model also involves a differential equation regulating the areal bacterial density σ_b on the bottom of the chamber:

$$\partial_t \sigma_b = \sigma_b \frac{c}{c_0 \tau}.$$

This equation assumes that the growth rate of bacteria is proportional to the oxygen concentration, as a means to hamper bacteria growth where oxygen is depleted. In the Comsol model, this areal density was replaced with a volumetric density $n_b = \sigma_b/h$ in the confined space, in order to have a full 3D model.

Conflicts of interest

There are no conflicts to declare.

Acknowledgements

This project has received funding from the European Research Council (ERC) under the European Union's Horizon 2020 Research and Innovation Programme (grant agreement no. 772725, project HiPhore).

Notes and references

- 1 F. Wu and C. Dekker, *Chem. Soc. Rev.*, 2016, **45**, 268–280.
- 2 W. Zhou, J. Le, Y. Chen, Y. Cai, Z. Hong and Y. Chai, *TrAC, Trends Anal. Chem.*, 2019, **112**, 175–195.
- 3 F. J. H. Hol and C. Dekker, *Science*, 2014, **346**, 1251821.
- 4 S. Kou, D. Cheng, F. Sun and I.-M. Hsing, *Lab Chip*, 2016, **16**, 432–446.
- 5 X.-Y. Zhang, K. Sun, A. Abulimiti, P.-P. Xu and Z.-Y. Li, *Micromachines*, 2019, **10**, 606.
- 6 A. Burmeister, F. Hilgers, A. Langner, C. Westerwalbesloh, Y. Kerkhoff, N. Tenhaef, T. Drepper, D. Kohlheyer, E. von Lieres, S. Noack and A. Grünberger, *Lab Chip*, 2018, **19**, 98–110.
- 7 J. Song, Y. Zhang, C. Zhang, X. Du, Z. Guo, Y. Kuang, Y. Wang, P. Wu, K. Zou, L. Zou, J. Lv and Q. Wang, *Sci. Rep.*, 2018, **8**, 6394.
- 8 M. M. Salek, F. Carrara, V. Fernandez, J. S. Guasto and R. Stocker, *Nat. Commun.*, 2019, **10**, 1877.
- 9 N. Tandogan, P. N. Abadian, S. Epstein, Y. Aoi and E. D. Goluch, *PLoS One*, 2014, **9**, e101429.
- 10 L. Tweedy, P. A. Thomason, P. I. Paschke, K. Martin, L. M. Machesky, M. Zagnoni and R. H. Insall, *Science*, 2020, **369**, 6507.
- 11 P. Wang, L. Robert, J. Pelletier, W. L. Dang, F. Taddei, A. Wright and S. Jun, *Curr. Biol.*, 2010, **20**, 1099.
- 12 D. Yang, A. D. Jennings, E. Borrego, S. T. Retterer and J. Männik, *Front. Microbiol.*, 2018, **9**, 871.
- 13 F. Si, B. Li, W. Margolin and S. X. Sun, *Sci. Rep.*, 2015, **5**, 11367.
- 14 J. Männik, R. Driessen, P. Galajda, J. E. Keymer and C. Dekker, *Proc. Natl. Acad. Sci. U. S. A.*, 2009, **106**, 14861–14866.
- 15 Y.-J. Eun, P.-Y. Ho, M. Kim, S. LaRussa, L. Robert, L. D. Renner, A. Schmid, E. Garner and A. Amir, *Nat. Microbiol.*, 2018, **3**, 148–154.
- 16 J.-J. Bourgois, F. E. Sluse, F. Baguet and J. Mallefet, *J. Bioenerg. Biomembr.*, 2001, **33**, 353–363.
- 17 T. E. Riedel, W. M. Berelson, K. H. Nealson and S. E. Finkel, *Appl. Environ. Microbiol.*, 2013, **79**, 4921–4931.

